Q. J. R. Meteorol. Soc. (1988), **114**, pp. 1517–1534 551.465

On the recirculation of the subtropical gyre

By JOHN MARSHALL and GEORGE NURSER
Space and Atmospheric Physics Group, Imperial College, London

(Received 7 April 1987; revised 29 June 1988)

SUMMARY

A hydrographic section through the Gulf Stream and its recirculation to the south is interpreted in terms of an analytical model based on the baroclinic Fofonoff gyre, in which layers shielded from forcing are homogenized to a uniform value of potential vorticity. Given this simple paradigm of the circulation, the process of anticyclogenesis is studied in which seasonal changes in the volume of low potential vorticity waters accompany a steepening of the main thermocline and an intensification of the recirculating gyre. The consequences of the gyre intensification for the structure of the bowl, the circulation within it and the deep abyssal flow are investigated. It is shown that as the anticyclogenesis proceeds, there is a general southward shift of the current systems; the bowl of the circulation strikes the ocean floor further south and there is an intensification of the depth-independent recirculation tight in to the axis of the Stream. These changes in the structure of the recirculation are broadly in accord with observed seasonal variability associated with winter-time mode water production.

1. INTRODUCTION

The Gulf Stream extension and its recirculation to the south is a region whose dynamics are of great interest. Here in the north-west corner of the subtropical gyre the Sverdrup constraint on the integrated mass transport no longer holds: the circulation is 'overspun' with inertial effects exerting a controlling influence. The presence of the intense eastward flowing Gulf Stream extension, on the northern rim of the gyre, see Fig. 1, is an indication of the inertial nature of the flow.

Warm fluid emanating from the western boundary current flows eastwards in this jet and, in winter, yields up much heat to the atmosphere. The consequent convection weakens the stratification and so can act as a vertically distributed source of low potential vorticity on the northern rim of the gyre. The direct driving by the wind must also be an important vorticity sink; as noted by Behringer *et al.* (1979) the eastward wind-stress is particularly intense over the warm core of the Gulf Stream in winter and its curl is high and anticyclonic. Thus the recirculation occurs where fluid circulating in the gyre is very likely to have its potential vorticity reduced by both thermodynamic and mechanical surface processes.

Following a severe winter the volume of low potential vorticity (weakly stratified) 'mode' waters increases (McCartney *et al.* 1980) and the anticyclonic recirculation is observed to strengthen—this intensification of the Gulf Stream has been termed 'anti-cyclogenesis' by Worthington (1972, 1976). In the hydrographic data he found a prominent seasonal cycle in the Gulf Stream transport east of Cape Hatteras with a maximum in early spring and a minimum in late autumn. Recent observational evidence documenting the spring-time intensification of the Gulf Stream can be found in hydrographic measurements presented by Halkin and Rossby (1985) and the satellite altimetric measurements of Fu *et al.* (1986). The latter study is particularly significant because it provides a completely independent measure of seasonal variability based on six years of altimetric measurements of sea surface height.

The reduction of potential vorticity in the upper waters to create the mode waters is observed to be associated with substantial deepening of the surface layer, a steepening of the downward slope of the main thermocline and an increase in the transport of the Gulf Stream. This led Worthington (1976) to speculate that the mode water formation drove the gyre intensification. However, any such causal relationship remains unproven.

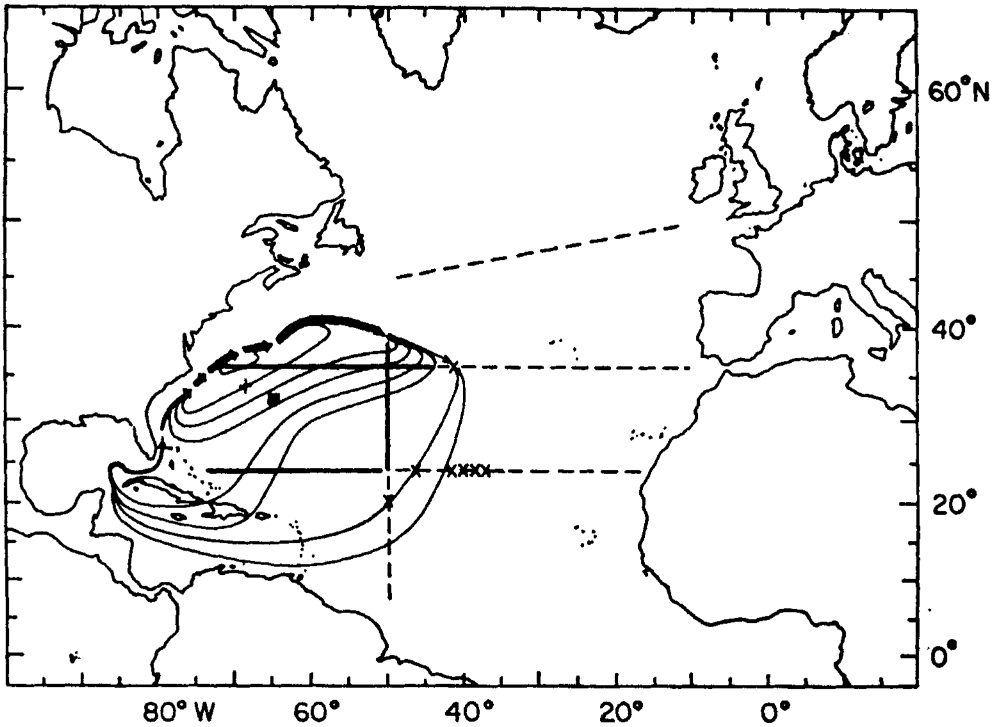

Figure 1. Warm water (>17°C) circulation diagram of Worthington (1976, Fig. 42). The solid segments of section lines indicate the location of a strong continuous potential vorticity minimum layer near $\sigma = 26{\cdot}5\ \mathrm{mg\,cm^{-3}}$, and therefore the main recirculation of eighteen-degree water.

In this study the mechanism responsible for the gyre intensification is not considered, but rather we enquire into its consequences for the structure of the main thermocline beneath the mode water wedge and for the deep abyssal flows documented by Schmitz (1980). Since the recirculation is not well described by models constrained to be in Sverdrup balance, instead the baroclinic Fofonoff gyre considered in Marshall and Nurser (1986)—hereafter MN—is adopted as a paradigm of the circulation. MN attribute the fundamental structure (both in the vertical and the horizontal) of the Gulf Stream extension and its recirculation to the tendency for potential vorticity to be constant along streamlines. They construct analytical solutions, baroclinic generalizations of Fofonoff's (1954) barotropic gyres, which bear a striking resemblance to the recirculation. Since such steady, free solutions exist, they can be resonantly forced; here it is suggested that anticyclogenesis is a 'resonance' of these nonlinear free modes excited by sources of low potential vorticity in the north-west corner of the gyre. An important element of the mechanism is the trapping of fluid parcels by closed potential vorticity contours in the recirculation. Fluid can thus recirculate many times with its potential vorticity being set by integral balances between mechanical and thermodynamical processes.

In section 2 the major features of the recirculation, as revealed by its hydrography, are reviewed and interpreted dynamically. In section 3 we describe a three-layer quasi-geostrophic model of the recirculation and consider how changes in the slope of the main thermocline influence the flow beneath, including the deep abyssal flow. Particular attention is focused on the weakly depth-dependent flows which make up the recirculation on the southern flank of the separated Gulf Stream.

2. THE RECIRCULATION AND ITS DYNAMICS

(a) *Observations*

Figure 1 shows the circulation pattern deduced by Worthington (1976) for waters warmer than 17 °C. The Gulf Stream runs along the northern rim of the warm water lens and the water then recirculates to the south. It has been estimated (see the summary of observations in Richardson (1985)) that of the 140 Sverdrups flowing eastward in the Gulf Stream extension perhaps 4/5 is recirculating. The major part of the transport of the Gulf Stream is in fact eighteen-degree water (sometimes called mode water), characterized by its weak stratification and hence anomalously low values of potential vorticity. McCartney (1982) has used this characteristic to map the spatial distribution of these waters. An important process in the formation of mode water is the convective overturning of the top few hundred metres of water along a 2000 km stretch just south of the Gulf Stream front. This convectively tainted water is formed locally and advected away laterally in the recirculating gyre; it moves southwards and is released into the thermocline forming a bolus of weakly stratified water. The formation region is small compared with the horizontal extent over which mode water is found. The solid segments of the section lines in Fig. 1 indicate the existence of a continuous potential vorticity minimum. Figure 2, a north/south section along 50°W, indicates the vertical and horizontal extent of mode waters—they appear as a thickening of isentropic layers, a 'wedge' centred on $\sigma = 26{\cdot}5$ in Fig. 2(a), characterized by anomalously low values of potential vorticity $q = -f\partial\rho/\partial z$ in Fig. 2(b). Above the wedge is the weak, seasonal pycnocline, below is the main pycnocline.

We assume that the flow transverse to the section is in thermal wind balance. Associated with the recirculating, westward flowing waters south of the Gulf Stream, the pycnocline slopes downwards to the north and then sharply upwards at the Gulf Stream front (39°N) as the flow is returned eastward in a narrow interior jet (the vertical dotted line in Fig. 2 indicates the southern edge of the Stream).

There is evidence of a bowl in Fig. 2(a) (its estimated position is indicated by the thick line) within which the flow is much stronger than outside where the isopycnals flatten out. Figure 2(b) suggests that potential vorticity is more uniform within this bowl than outside it (the homogenization of Rhines and Young (1982)). Outside the bowl, q reverts back to its reference value, set by the planetary vorticity and the reference stratification. Bower *et al.* (1985) present evidence that at depth tracers (O_2 and q) are uniform across the axis of the Stream. This suggests that the deeper part of the gyre, shielded from atmospheric forcing, adopts the value of q found at its northern rim (see also dynamical arguments presented in Rhines and Young (1982) and Nurser (1988)).

Following a severe winter a contraction of the gyre may occur in which, together with a reduction in the potential vorticity of upper layer light waters, the Gulf Stream front migrates southwards and the thermocline deepens near the front. This results in an increase in the strength of the circulation: the anticyclogenesis documented by Worthington (1976). Figure 3, taken from Worthington, shows schematically the change in the Gulf Stream position and interface slope before and after such a winter. What seems to be clear from the observations is that variations in the depth-integrated baroclinic transport come about through variations in the shear beneath the thermocline: an increase in the depth of isopycnals on the Sargasso Sea side of the Stream which appears to track with eighteen-degree water formation (McCartney; private communication). Worthington (1977), comparing Gulf Stream temperatures before and after cold air outbreaks, finds that before a cold winter 18° water is found only to a depth of 400 m; after a cold winter it penetrates to 600 m. Indeed Worthington (1982) observes that the greatest depth

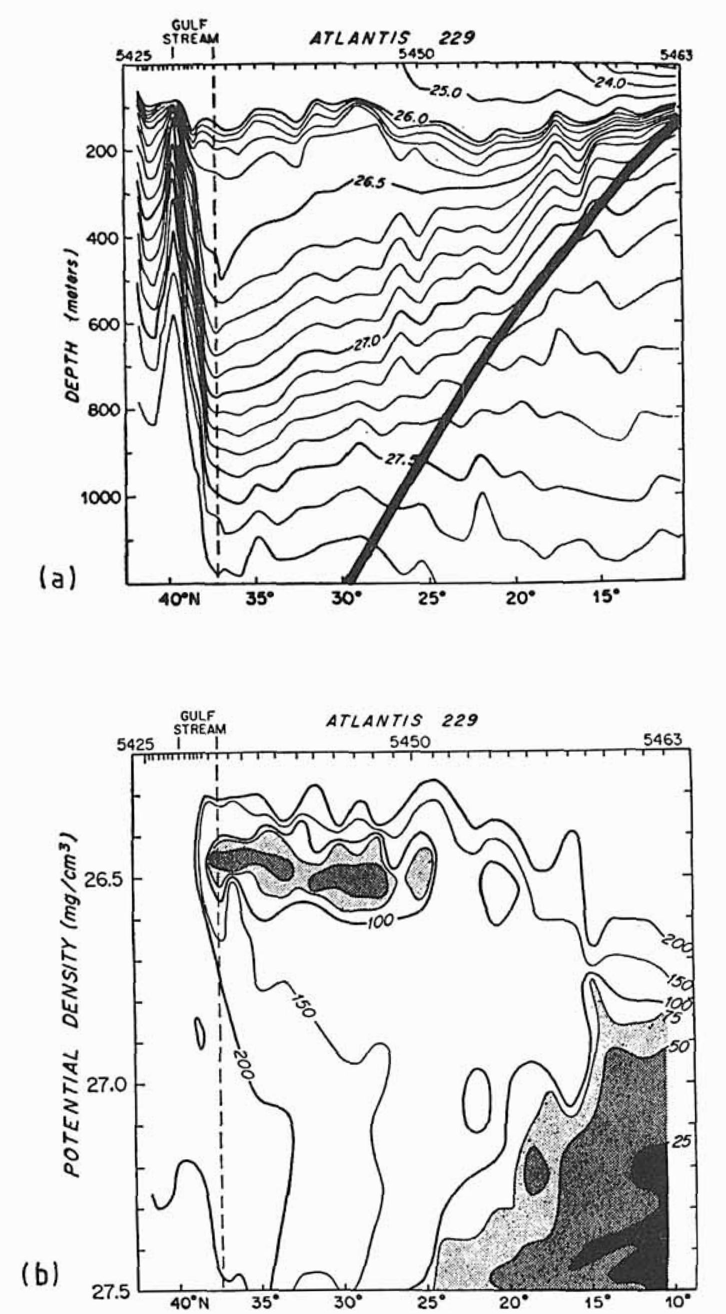

Figure 2. Property sections for a section along 50°W made by RV *Atlantis* in 1956, between November 13 (north) and November 30 (south) taken from McCartney (1982). The section location is indicated on Fig. 1. The eastward flow of the Gulf Stream lies between stations 5432 (39° 37′N) and 5439 (37° 16′N). The vertical dashed line marks the southern edge of the Gulf Stream: the dynamic height maximum occurs at station 5439. (a) Potential density σ (in $\mathrm{mg\,cm^{-3}}$, depth as ordinate): eighteen-degree water marked by larger isopycnal spacing centred at $\sigma = 26{\cdot}5\,\mathrm{mg\,cm^{-3}}$. The thick line marks the 'bowl' within which potential vorticity shows little variation. (b) Potential vorticity (in $10^{-14}\mathrm{cm^{-1}s^{-1}}$) with potential density as ordinate. Shading has been chosen to emphasize the low potential vorticity water masses: single, double and triple intensity denoting respectively, less than 75, 50 and $25\times10^{-14}\mathrm{cm^{-1}s^{-1}}$. The potential vorticity minimum layer centred near $\sigma = 26{\cdot}5\,\mathrm{mg\,cm^{-3}}$ represents the eighteen-degree water.

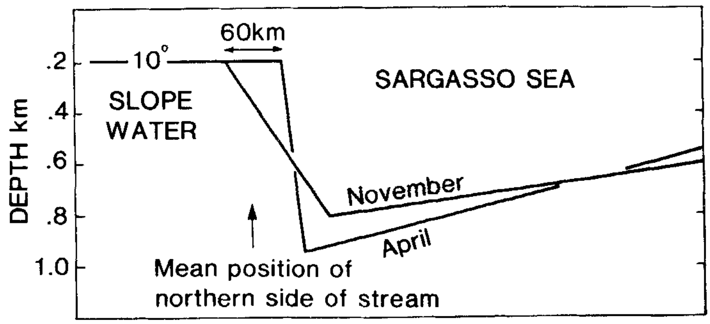

Figure 3. A schematic illustration of annual changes in Gulf Stream position and interface shape. From Worthington (1976).

of the main thermocline south of the Gulf Stream is *always* found beneath the deepest mixed layer of 18° water; this greatest thermocline depth represents the centre of the Gulf Stream anticyclone.

We reiterate, however, that the sense or even the existence of any causal relationship between the formation of mode waters and intensification of the circulation remains unclear. Indeed Woods and Barkmann (1985) argue that the volume of mode water is *controlled by* the strength of the circulation.

Before going on to a dynamical interpretation of the hydrographic section, Fig. 2, one should remember that it only reveals the baroclinic component of the flow and cannot be used unambiguously to infer absolute velocities. Some of the difficulties inherent in budgeting for absolute transports from hydrography alone, based on a level of no motion hypothesis, can be seen in the study of Luyten and Stommel (1982). To ensure a net mass balance across the 50°W section they introduce a barotropic (depth-independent) component recirculating south of the Stream. Direct current measurements reported in, for example, Schmitz (1980) and Richardson (1985), show that indeed, tight in to the axis of the Stream, barotropic components exist reaching magnitudes of perhaps 10 cm s^{-1}. These appear as deep counter-currents on each flank of the Stream. Abyssal counter-rotating gyres are also evident in the current measurements described by Hogg (1983) and the tracer distributions and further current measurements presented in Hogg *et al.* (1986). They appear to have a meridional scale of perhaps two or three hundred kilometres.

(*b*) *A dynamical interpretation*

MN liken the circulation revealed in Figs. 1 and 2 to baroclinic Fofonoff gyres and, within the constraints of quasi-geostrophy, solve for cases in which potential vorticity is uniform within the main thermocline. In MN these solutions were developed as an extension of homogeneous ocean circulation theory to a baroclinic ocean (for a review of the homogeneous theory see Marshall (1986)). Here, however, the problem is approached from a slightly different perspective which makes the link with hydrographic sections more explicit. Rather than making the quasi-geostrophic assumption and so being limited to small layer depth changes, the thermocline equations are adopted in a continuously stratified model (see Nurser (1988) for more details of the continuously stratified thermocline model and Greatbatch (1987) for a continuously stratified quasi-geostrophic MN model). However, in section 3 we readopt the quasi-geostrophic framework for analytical convenience—no essential dynamics is lost and solutions can be obtained without neglecting relative vorticity.

Let us suppose that the most important effect of the thermodynamical/dynamical processes in the upper waters of the recirculation (the top 200 m say), so far as the structure of the flow beneath is concerned, is to depress the main thermocline. It will thus be assumed that the depth of the $\sigma = 26{\cdot}6$ surface is known and we shall enquire into the consequences for the flow beneath. Then, if, as suggested by the observations, it is assumed that where there is flow beneath, the potential vorticity is uniform and furthermore equal to its value at the axis of the Stream, the shape and depth of the 'bowl' within which the circulation is confined is set and can be easily found.

Suppose that the 'bowl' is of depth $D \equiv D(y)$—outside the bowl the isopycnals are horizontal and there is no flow (see Fig. 4). Within the bowl the isopycnals slope—$h \equiv h(y)$ is the depth of the $\sigma = 26{\cdot}6$ surface, say, in Fig. 2(a). At latitudes where h reverts back to its undisturbed depth h_1 the stratification is given by $\rho = \rho_0(z)$ (or alternatively $z = z_0(\rho)$).

Referring to the schematic diagram, Fig. 4, of the 50°W section, our objective is to relate D to h, and solve for the flow within the bowl.

Now

$$\int_{\rho(-D)}^{\rho(-h)} (\partial z/\partial \rho) d\rho = \int_{-D}^{-h} dz = D - h \tag{1a}$$

integrating from the bowl up to the bottom of the mode water wedge. Provisionally we

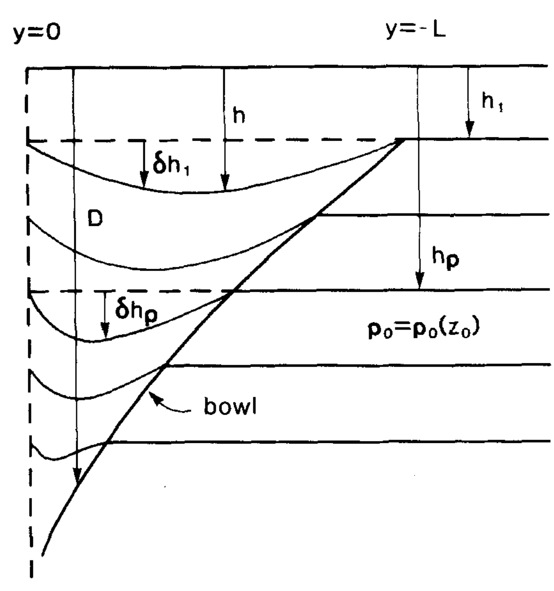

Figure 4. A schematic representation of the hydrographic section, Fig. 2, showing the bowl of the circulation at depth $D(y)$, within which the circulation is confined. Outside the bowl there is no flow and isopycnals are horizontal.

shall neglect the relative vorticity and so $\partial z/\partial \rho$ can be expressed in terms of the potential vorticity thus

$$q = -f\partial\rho/\partial z = -\frac{f}{\partial z/\partial\rho}$$

and the left-hand side of Eq. (1a) can be written

$$\int_{\rho(-D)}^{\rho(-h)} \frac{\partial z}{\partial\rho} d\rho = -\int_{-D}^{-h_1} \frac{f}{q}\frac{d\rho}{dz_0} dz_0.$$

Now it is assumed that:

(1) within the bowl, $-D < z < -h$, q is constant; and further

(2) within the bowl q is given by the reference stratification attained along $f = f_0$ at the axis of the Stream where $h = h_1$, i.e.

$$q = q_0 = -\frac{f_0}{\partial z_0/\partial\rho}$$

and so it follows that

$$\int_{\rho(-D)}^{\rho(-h)} (\partial z/\partial\rho)d\rho = \int_{-D}^{-h_1} (f/f_0)dz_0 = (f/f_0)(D - h_1). \tag{1b}$$

Combining Eqs. (1a) and (1b) gives our required relationship

$$D - h = (f/f_0)(D - h_1) \qquad \text{or} \qquad D - h_1 = (f_0/(f_0 - f))\delta h_1 \tag{2}$$

where δh_1 is the deviation of our reference density surface from its equilibrium depth. For an alternative derivation of Eq. (2) see Nurser (1988). The δh_ρ, the deviations of the isopycnals from their reference depths h_ρ within the bowl, can also be calculated and are given by

$$\delta h_\rho = \delta h_1 - (1 - f/f_0)(h_\rho - h_1). \tag{3}$$

Equations (2) and (3) are merely a consequence of the uniformity of q in the bowl. Equation (2) predicts for the depth of penetration of the bowl in terms of the thickness of the surface layer; Eq. (3) predicts for the structure of the main thermocline and therefore the circulation within the bowl. The controlling parameter is δh_1.

These equations can be used diagnostically to enquire into the consequences of a gyre contraction on the vertical structure of the gyre. As the winter proceeds, Fig. 4, δh_1 increases and, through Eq. (2), it can readily be seen that the depth of penetration of the bowl increases. In an infinitely deep ocean this hyperbolic plunge of our homogenized gyre would be arrested since the relative vorticity contribution to q (due to horizontal shear) would play its part in maintaining a uniform potential vorticity as the axis of the Stream is approached, allowing a thinning of isopycnal layers (see section 3(*b*)). Eventually isopycnal surfaces must begin to bow upwards as the recirculating waters are swept eastwards again in the Gulf Stream current on the northern rim of the gyre.

It is instructive to estimate the depth to which the circulation penetrates in the 50°W section (Fig. 2), by making use of Eq. (2). Concentrating on the $\sigma = 26{\cdot}6$ surface we estimate that at 30°N it is some 250 m deeper than its reference depth of 200 m at 15°N.

Thus taking $\delta h_1 = 250\,\mathrm{m}$ and the axis of the Stream to be at 40°N, Eq. (2) gives

$$(D - h_1)_{30°\mathrm{N}} = \frac{\sin 40°}{\sin 40° - \sin 30°} \times 250 \sim 1200\,\mathrm{m}$$

in approximate agreement with the depth of the bowl at 30°N suggested by Fig. 2.

As the axis of the Stream is approached, however, δh_1 increases and $f \rightarrow f_0$. Assuming that indeed $q = q_0$ in the homogenized gyre, then Eq. (2) holds and, irrespective of the detailed variation of δh_1, D must become a strong function of latitude and increase in a roughly hyperbolic manner (until the Stream is actually reached, whereupon δh_1 declines sharply). For a δh_1 of 300 m, D becomes equal to the depth of the ocean, taken to be 4500 m, at a latitude of about 37°, some 300 km south of the Stream. It should be emphasized that these estimates are sensitive to the assumed value of q in the homogenized gyre (numerical inversions carried out by N. Hall (private communication) suggest that the depth of penetration of the gyre is less marked if values of q higher than q_0 are assumed, as suggested by the 50°W section).

On balance, however, it seems likely that the bowl does strike the ocean floor some distance south of the Gulf Stream. Between this latitude and the axis of the Stream, we shall see that a barotropic circulation can exist, driven by eddies and retarded by bottom friction.

This is our model's representation of the barotropic core of the recirculation seen in the observations (Richardson 1985) and eddy-resolving circulation models (Schmitz and Holland 1986). Relative vorticity makes a non-negligible contribution to q here, and is included in the three-layered quasi-geostrophic model considered in section 3.

Finally we note that if the circulation implied by Eq. (3) is closed by western, northern and eastern boundary currents the baroclinic generalizations of Fofonoff gyres are obtained, discussed in the context of quasi-geostrophic theory by MN. A plan view of such a gyre with inertial boundary layers appended is shown in Fig. 5. The eastern boundary layer is an unrealistic feature of the model and is best regarded as a device to ensure mass balance; it represents the complex time-dependent motions which in reality

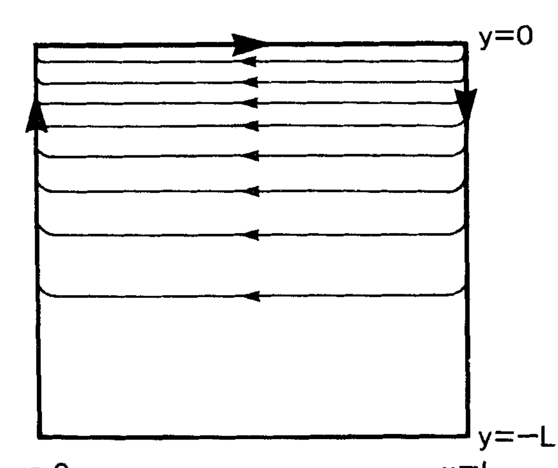

Figure 5. A horizontal section through a baroclinic Fofonoff gyre. In the interior where relative vorticity is negligible the flow is along latitude circles; in the inertial boundary currents relative vorticity allows the potential vorticity contours and hence the flow to run parallel to the coast. The analogue of the separated Gulf Stream seen in Fig. 1 runs along the northern wall.

allow the circulation to be completed. The solution sketched in Fig. 5 is one in which potential vorticity is constant along streamlines. Here it is proposed that Worthington's anticyclogenesis is a resonant forcing of these nonlinear free modes which are 'spun-up' by sources of low potential vorticity in the north-west corner of the gyre.

3. A THREE-LAYER MODEL OF THE SUBTROPICAL RECIRCULATION

Marshall and Nurser (1986) obtained a series of Fofonoff gyres 'stacked' one on top of the other circulating as pools of uniform potential vorticity. Just as in the continuously stratified model discussed in section 2, where the latitudinal extent of the homogenized pool becomes ever more restricted with depth (the problem of solving for the bowl of the circulation, D in Fig. 4) so, in the layered model, flow in the nth layer is confined north of a latitude denoted by l_n which is further north the deeper the layer considered. South of this latitude q contours cannot close on themselves—they intersect the lateral boundaries disallowing flow. As in section 2, the latitudes l_n are determined by assuming that the potential vorticity is uniform within the gyre and equal to its value at the northern rim of the gyre.

In this section the $2\frac{1}{2}$-layer model of MN is extended to consider Fofonoff gyres in a three-layer model. A schematic diagram showing the vertical structure of the model is shown in Fig. 6(a). The top layer is imagined to be made up of mode water exposed to surface processes, representing the 'wedge' in Fig. 2(a). The middle layer represents the main thermocline within which potential vorticity is supposed uniform. The bottom layer extends to the ocean floor. A plan view of the basin is shown in Fig. 6(b)—note that $y = 0$ is the northern edge of the gyre.

In a Fofonoff gyre the potential vorticity is linearly related to the streamfunction: thus we have

$$q_1 = \beta y + F(\psi_2 - \psi_1) + \nabla^2\psi_1 = C_1\psi_1 - \beta L; \qquad -L < y < 0 \tag{4a}$$

$$q_2 = \beta y + F(\psi_1 - 2\psi_2 + \psi_3) + \nabla^2\psi_2 = 0; \qquad -l_2 < y < 0 \tag{4b}$$

$$q_3 = \beta y + \alpha F(\psi_2 - \psi_3) + \nabla^2\psi_3 = C_3\psi_3; \qquad -l_3 < y < 0 \tag{4c}$$

with C_1 and C_3 constants.

The quasi-geostrophic potential vorticity and the quasi-geostrophic streamfunction in the three layers are denoted by q_i and ψ_i respectively; β is the planetary vorticity gradient and L the north–south extent of the gyre. For convenience it has been assumed that the density jumps between each successive layer are equal and that the upper two layers are of equal depth, $H_1 = H_2$ at $y = -L$; the ratio of the depth of the upper two layers to the depth of the deep abyssal layer is $\alpha = H_1/H_3$. The inverse of the square of a (Rossby) length scale is $F = L_\rho^{-2} = f_0^2/(g'H)$, where g' is the reduced gravity and f_0 is the Coriolis parameter.

The latitudes l_2 and l_3, which define the meridional extent of the flow in layers two and three, are to be determined.

As described in detail in MN, the constants C_i in Eqs. (4) are set by integral balances between potential vorticity sources and sinks over the gyre—see Eq. (2.5) of MN. If in the upper layer potential vorticity sources (diabatic or mechanical) are balanced by lateral downgradient transfer of potential vorticity then it may be deduced that $C_1 < 0$; if in the bottom Ekman layer frictional dissipation of potential vorticity is balanced by eddy transfer then it may be deduced that $C_3 > 0$; in the middle layer, shielded from sources and sinks, eddies erode the potential vorticity gradient, C_2 is zero and q_2 uniform. We will find that C_1 controls the strength of the shear in the upper thermocline and C_3 the strength of the barotropic component of the circulation.

Finally it should be noted that the constant $-\beta L$ in Eq. (4a) ensures that q_1 is continuous across the southern edge of the gyre at $y = -L$. It leads to a discontinuity in q_1 at the latitude of the separated Gulf Stream, a feature of the observed potential vorticity field in the upper mid-thermocline of the North Atlantic.

We now go on to find solutions to Eqs. (4) appropriate to regions far from eastern or western boundaries where we may assume $\partial/\partial x = 0$ and replace ∇^2 by $\partial^2/\partial y^2$.

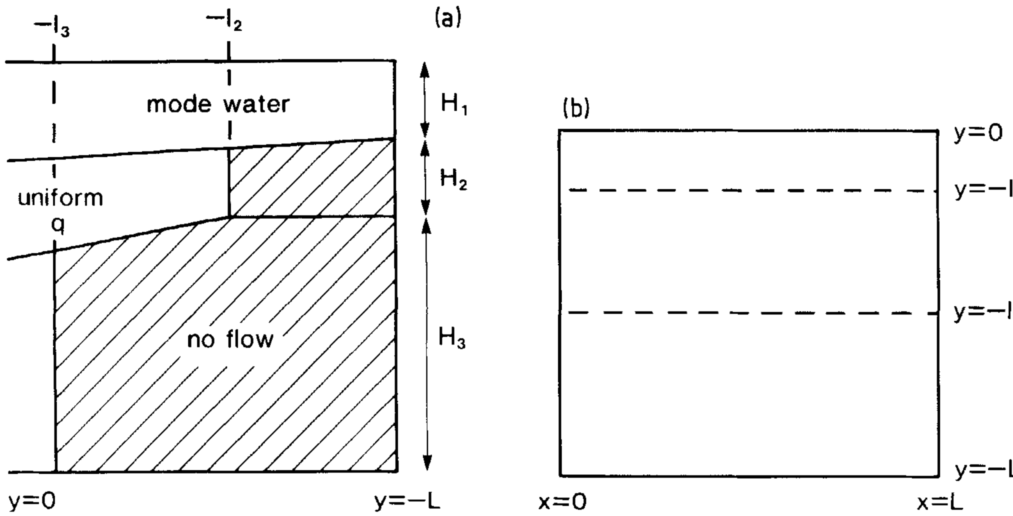

Figure 6. (a) A meridional section through the three-level model showing its vertical structure. The meridional extent of the flow in layers two and three is confined north of $y = -l_2$ and $y = -l_3$, respectively; south of these latitudes there is no flow. (b) A plan view of the gyre.

(a) *The solution south of $y = -l_3$*

In the interior of the flow away from boundary currents the contribution of the relative vorticity to the potential vorticity in Eqs. (4) can be neglected. Furthermore, south of the latitude l_3 (outside the bowl) there can be no flow in the lower layer because q_3 contours intersect the lateral boundary: $\psi_3 = 0$ in Eqs. (4) and the interior solution is identical to that found in the $2\frac{1}{2}$-layer model of MN. It can be readily shown (see MN, Eq. (3.8) and Eq. (3.17)) that

$$\left.\begin{aligned} \psi_{I1} &= \beta(y+L)/(C_1+F) \\ \psi_{I2} &= 0 \\ \psi_{I3} &= 0 \end{aligned}\right\} \qquad -L < y < -l_2 \tag{5a}$$

$$\left.\begin{aligned} \psi_{I1} &= \beta(3y+2L)/(F+2C_1) \\ \psi_{I2} &= \beta\{y(2F+C_1)+FL\}/\{F(2C_1+F)\} \\ \psi_{I3} &= 0 \end{aligned}\right\} \qquad -l_2 < y < -l_3 \tag{5b}$$

where

$$l_2 = FL/(C_1+2F). \tag{5c}$$

In the $2\frac{1}{2}$-layer model of MN the latitude l_3 did not appear because the third layer was infinitely deep. However, the existence in the three-layer model of a third layer of finite depth admits the possibility of closing off q contours in the third layer and hence allowing non-zero values of l_3 with abyssal flow north of $y = -l_3$. Given the solution south of $y = -l_3$, Eqs. (5a) and (5b), the latitude l_3 can be calculated from Eq. (4c) by assuming that q_3 is continuous across $y = -l_3$ and noting that outside the bowl $\psi_3 = 0$. It may be deduced that

$$l_3 = \alpha FL/\{C_1(2+\alpha) + F(1+2\alpha)\}. \tag{5d}$$

Note that when $\alpha = 0$ the lower layer is infinitely deep, $l_3 = 0$, and our problem reduces to that considered in MN. It is worthy of note that l_3 is independent of C_3.

To calculate the ψ_3 field where all layers are moving, a more systematic approach is adopted.

(b) The solution north of $y = -l_3$

Writing Eqs. (4) in vector form then we have, replacing ∇^2 with $\partial^2/\partial y^2$

$$\mathbf{b} + F^{-1}\,\partial^2\boldsymbol{\psi}/\partial y^2 = \mathbf{A}\boldsymbol{\psi} \tag{6}$$

where

$$\mathbf{b} = F^{-1}\begin{pmatrix}\beta(y+L)\\ \beta y\\ \beta y\end{pmatrix},\qquad \boldsymbol{\psi} = \begin{pmatrix}\psi_1\\ \psi_2\\ \psi_3\end{pmatrix},$$

$$\mathbf{A} = \begin{pmatrix}1+C_1' & -1 & 0\\ -1 & 2 & -1\\ 0 & -\alpha & \alpha + C_3'\end{pmatrix}$$

and $C_1' = C_1/F$, etc. Solutions of Eq. (6) may be found by summing the particular integral, the interior solution $\boldsymbol{\psi}_{\mathrm{I}}$ satisfying

$$\mathbf{A}\boldsymbol{\psi}_{\mathrm{I}} = \mathbf{b} \tag{7}$$

and the complementary function, the boundary correction $\boldsymbol{\psi}_{\mathrm{B}}$, satisfying

$$F^{-1}\partial^2\boldsymbol{\psi}_{\mathrm{B}}/\partial y^2 = \mathbf{A}\boldsymbol{\psi}_{\mathrm{B}} \tag{8}$$

where $\boldsymbol{\psi} = \boldsymbol{\psi}_{\mathrm{I}} + \boldsymbol{\psi}_{\mathrm{B}} = \mathbf{0}$ at $y = 0$ is a boundary condition for Eq. (6).

If $\det\mathbf{A} = 0$, Eq. (6) must be solved directly for the total $\boldsymbol{\psi}$: this case is discussed along with the complementary function in section 3(*b*)(ii).

The solutions to Eq. (7) and Eq. (8) are now considered in turn.

(i) *The particular integral.* Inverting Eq. (7) for ψ_{I} gives

$$\left.\begin{aligned}\psi_{\mathrm{I}1} &= (\beta/F\Delta)\{(2\alpha + 3C_3' + 1)y + (\alpha + 2C_3')L\}\\ \psi_{\mathrm{I}2} &= (\beta/F\Delta)\{[2\alpha + 1 + (1+\alpha)C_1' + 2C_3' + C_1'C_3']y + (\alpha + C_3')L\}\\ \psi_{\mathrm{I}3} &= (\beta/F\Delta)\{[2\alpha + 1 + (\alpha+2)C_1']y + \alpha L\}\end{aligned}\right\} \tag{9}$$

provided that $\Delta > 0$, where $\Delta = \det\mathbf{A} = \alpha C_1' + C_3' + 2C_1'C_3'$.

The solution Eq. (9) is the sum of a barotropic (depth-independent) and baroclinic component; flow is to the west supporting inertial boundary layers provided that

$$-\tfrac{1}{2} < C_1' < 0 \tag{10}$$

$$\det\mathbf{A} > 0. \tag{11}$$

However, the solution (9) is physically relevant only if the complementary function ψ_B is confined to a boundary layer whose width is less than that of the recirculation. As will be seen in section 3(*b*)(ii) a necessary and sufficient condition for this confinement is that λ_1, the smallest eigenvalue of **A**, should satisfy $\lambda_1 \gg l_3^{-2}F^{-1} = L_\rho^2/l_3^2$. This condition may be violated because of the opposite signs of C_1 (negative) and C_3 (positive) implied by the forcing and dissipation integrals. Then the complementary function is important over the whole extent of the deep recirculation; indeed for $\Delta = 0$ the solution (9) does not even exist and the total ψ must be evaluated by direct solution of Eq. (6).

Immediate inspection of Eqs. (9) is useful, however, if det**A** is (algebraically) large enough for the complementary function to be confined; in this case the following limit cases are of interest.

(1) $C_3 \to \infty$. As C_3 becomes large the solution tends to that of the $2\frac{1}{2}$-layer model, Eqs. (5), in the case $C_1 = 0$: infinite bottom friction arrests the flow in the third layer north of $y = -l_3$. There is no barotropic component. A meridional section showing the isopycnal displacements and velocities normal to the section is plotted in Fig. 7(a) (the inertial boundary layer on the northern rim of the gyre has not been represented). Velocities are in units of βL_ρ^2 and so for a Rossby radius of 30 km and $\beta = 2 \times 10^{-11}\mathrm{m^{-1}s^{-1}}$, a non-dimensional speed of unity corresponds to a current of $1{\cdot}8\,\mathrm{cm\,s^{-1}}$.

(2) $C_1 \to 0$. As C_1 approaches zero the potential vorticity in the upper layer tends to a uniform value of $-\beta L$. The solution consists of the $2\frac{1}{2}$-layer baroclinic component, Eqs. (5), together with a barotropic component in the region north of $y = -l_3$, where now l_3 is given by $l_3 = \alpha L/(1 + 2\alpha)$.

For an α of 1/8 corresponding to upper layers of depth 500 m and an abyssal layer of 4000 m, $l_3 = L/10$ or 100 km if L is taken to be 1000 km. Thus the barotropic component is of confined meridional extent. A section through the gyre is plotted in Fig. 7(b) for the case $C_3' = 0{\cdot}4$: the flow south of $y = -l_3$ is as in Fig. 7(a) but north of $y = -l_3$ there is an additional barotropic component of strength $\beta(1 + 2\alpha)/(FC_3')$, inversely proportional to the magnitude of the bottom friction coefficient. It is this barotropic component that we identify with the tight recirculating gyre documented by, for example, Schmitz (1980). It is a consequence of the bowl hitting the ocean floor. Given the restricted meridional extent of the barotropic recirculation its form will be radically modified by relative vorticity which cannot be neglected north of $y = -l_3$.

This will be studied in section 3(*b*)(ii) where the structure of the boundary layers is found.

(3) $C_1 \to -F/2$. As C_1 becomes more negative the depth of the upper layer mode water wedge increases and penetrates to greater depth and, in our simple analytical model, this corresponds to the 'anticyclogenesis' described by Worthington.

As $C_1 \to -F/2$ the gyre spins up—the shear across the main thermocline is enhanced and the amplitude of the barotropic recirculation and its north–south extent increase: from Eq. (5c) and Eq. (5d), $l_3 \to l_2 \to -2L/3$ and the bowl of the gyre strikes the bottom further south. A north–south section across the gyre for the case $C_1' = -1/4$, $C_3' = 0{\cdot}4$ is shown in Fig. 7(c) and should be compared with Figs. 7(a) and 7(b). It can be seen that as C_1 becomes more negative, corresponding to an increase in the depth of the mode water, the shear across the main thermocline is enhanced and the latitude at which the bowl strikes the bottom migrates southwards; l_2 has increased from $L/2$ in Fig. 7(b) to $4L/7$ in Fig. 7(c): l_3 has increased from $L/10$ to $4L/23$. The meridional extent of the deep flow is thus enhanced.

It is also worthy of note that now, for non-zero C_1, the interface slopes are no longer

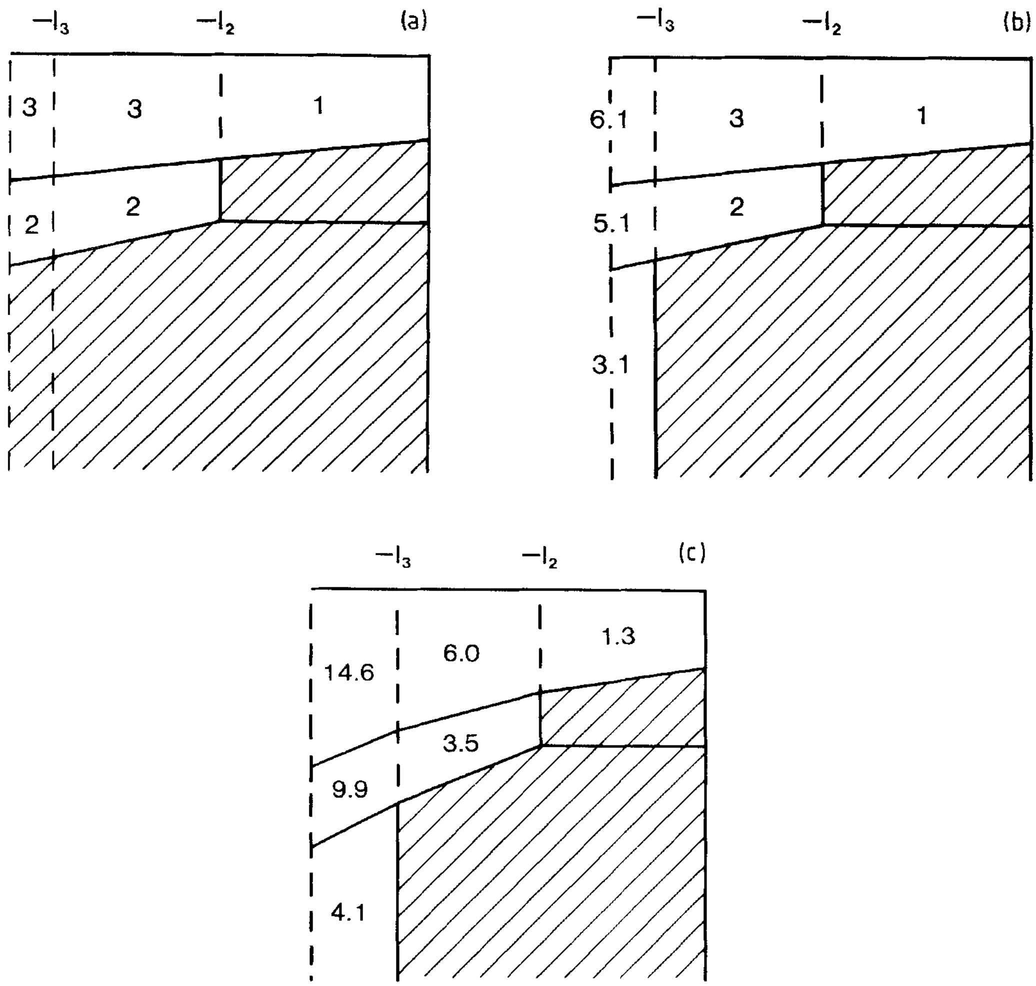

Figure 7. (a) The velocities normal to the section in each layer given by Eqs. (5) in the case $C_1' = 0$ (uniform potential vorticity) and $C_3' = \infty$ and $\alpha = 1/8$; in units of β/F. The latitude $l_2 = L/2$ and $l_3 = L/10$. Infinite bottom friction has arrested the flow north of $y = -l_3$. (b) The velocities normal to the section in each layer given by Eqs. (9) in the case $C_1' = 0$ and $C_3' = 0{\cdot}4$ and $\alpha = 1/8$; $l_2 = L/2$ and $l_3 = L/10$ as in (a). Now north of $y = -l_3$ there is a barotropic component of strength $(2\alpha + 1)/C_3$. (c) The velocities normal to the section in each layer given by Eqs. (9) in the case $C_1' = -0{\cdot}25$ (corresponding to anticyclogenesis) and $C_3' = 0{\cdot}4$ and $\alpha = 1/8$; $l_2 = 4L/7$ and $l_3 = 4L/23$. The westward interior velocities in each layer support inertial boundary currents. The meridional extent and strength of the barotropic recirculation have increased relative to (b) as has the strength of the baroclinic component. The interfacial slopes are no longer constant but steepen to the north.

constant but rather increase as the axis of the Stream is approached. This can easily be understood from Eq. (4a) since $\partial q_1/\partial y = C_1 U_1$. So as U_1 changes discontinuously at the latitudes l_n, so must $\partial q_1/\partial y$ to maintain a constant ratio C_1.

There is evidence from hydrographic sections—see for example Fig. 2—that the thermocline does indeed deepen rather rapidly just south of the axis of the Stream. That this occurs in our analytical model should, perhaps, be regarded as fortuitous since it is a consequence of the assumed constancy of C_1 in the upper layer.

As the anticyclogenesis proceeds and the gyre spins up, the shear across the main thermocline strengthens: it is very likely that the gyre equilibrates through vigorous lateral transfer of potential vorticity associated with enhanced baroclinic activity feeding off the available potential energy stored in the sloping isopycnals. Thus there is a governing mechanism: equilibration of the gyre can occur through lateral eddy transfer returning C_1 toward zero—the uniform q state. This suggests that the limit where C_1 is close to $-F/2$ is an unrealistic one.

Although we do not want to take any comparison with observations too far, our simple model does seem to mimic some features of the observed secular variability of the Gulf Stream and its recirculation. For example Schmitz and McCartney (1982) document changes in the observed structure of the recirculation that were associated with an increase in the volume of 18° water between October 1976 and April 1977, months which spanned the severe North American winter of 1976–1977. They describe a sharp increase in the vertical shear of the recirculation and a southward shift in the average current pattern in the thermocline south of the Stream, including a southward 'meander' of the abyssal currents.

(ii) *The complementary function.* The structure of the northern boundary layer current can most easily be studied by projecting the complementary function onto the eigenvectors of $\mathbf{A}$:

$$\boldsymbol{\psi}_{\mathrm{B}} = \sum_i \mathbf{e}_i \tilde{\psi}_{\mathrm{B}}^{(i)} \tag{12}$$

where the $\tilde{\psi}_{\mathrm{B}}^{(i)}$ are the expansion coefficients in terms of the eigenvectors of $\mathbf{A}$, $\mathbf{e}_i$ satisfying $\mathbf{A}\mathbf{e}_i = \lambda_i \mathbf{e}_i$. These $\tilde{\psi}_{\mathrm{B}}^{(i)}$ are given by $\tilde{\psi}_{\mathrm{B}}^{(i)} = \mathbf{e}_i^* \cdot \boldsymbol{\psi}_{\mathrm{B}}$ where $\mathbf{e}_i^*$, the left eigenvectors of $\mathbf{A}$, satisfy $\mathbf{e}_i^* \mathbf{A} = \lambda_i \mathbf{e}_i^*$ and are normalized such that $\mathbf{e}_i^* \cdot \mathbf{e}_j = \delta_{ij}$.

When $C_1 = C_3 = 0$, then $\mathbf{A}$ is just the operator representing the vortex-stretching in each layer and the eigenmodes $\mathbf{e}_i$ are the usual barotropic and baroclinic modes.

The $\tilde{\psi}_{\mathrm{B}}^{(i)}$ satisfy the equation

$$F^{-1} \frac{\partial^2}{\partial y^2} \tilde{\psi}_{\mathrm{B}}^{(i)} = \lambda_i \tilde{\psi}_{\mathrm{B}}^{(i)} \tag{13}$$

with boundary conditions

$$\tilde{\psi}_{\mathrm{B}}^{(i)} + \tilde{\psi}_{\mathrm{I}}^{(i)} = 0 \qquad \text{at } y = 0 \tag{14a}$$

where $\tilde{\psi}_{\mathrm{I}}^{(i)} = \mathbf{e}_i^* \cdot \boldsymbol{\psi}_{\mathrm{I}}$ (i.e. the axis of the Gulf Stream is a streamline) and

$$\tilde{\psi}_{\mathrm{B}}^{(i)} = 0 \qquad \text{at } y = -l_3 \tag{14b}$$

(i.e. the relative vorticity is zero on the southern flank of the inertial jet).

Solutions of exponential form (a confined jet) are only possible if all the λ_i are positive: this is assured if the coefficients I_i of the characteristic polynomial

$$\lambda^3 - I_1\lambda^2 + I_2\lambda - I_3 = 0$$

are all positive, where

$$I_1 = \mathrm{tr}\mathbf{A} = C_1' + C_2' + C_3'$$

$$I_2 = \tfrac{1}{2}\{(\mathrm{tr}\mathbf{A})^2 - \mathrm{tr}\mathbf{A}^2\} = 1 + 2\alpha + (2 + \alpha)C_1' + 3C_3' + C_1'C_3'$$

$$I_3 = \det\mathbf{A} = \alpha C_1' + C_3' + 2C_1'C_3'.$$

Westward flow at each level in the interior solution, Eqs. (9), is a necessary and sufficient condition, guaranteed if Eq. (11) is satisfied.

The width of the inertial jet is, from Eq. (13), $(\lambda_1 F)^{-1/2} = L_\rho \lambda_1^{-1/2}$ where λ_1 is the smallest eigenvalue of **A** and whose eigenmode is the 'pseudo-barotropic' mode, i.e. that which asymptotes to the barotropic mode $(1,1,1)^{\mathrm{T}}$ as C_1 and C_3 tend to zero. If this eigenvalue is small such that $|\lambda_1|^{1/2} \ll L_\rho/l_3$ then the pseudo-barotropic mode does not have boundary layer form and the solution for the total $\boldsymbol{\psi}$ does not depart far from that obtained by setting $\lambda_1 = 0$, corresponding to $\det\mathbf{A} = 0$. In this case the interior solution (9) does not exist and (6) must be found directly by projection onto the modes $\mathbf{e}_i$. We must then solve

$$\tilde{b}^{(i)} + F^{-1}\frac{\partial^2}{\partial y^2}\tilde{\psi}^{(i)} = \lambda_i \tilde{\psi}^{(i)} \tag{15}$$

where $\tilde{b}^{(i)}, \tilde{\psi}^{(i)} = \mathbf{e}_i^* \cdot \mathbf{b}, \mathbf{e}_i^* \cdot \boldsymbol{\psi}$ and the pseudo-barotropic eigenvalue $\lambda_1 = 0$.

Equation (15) for the pseudo-barotropic mode, which gives rise to a $\tilde{\psi}^{(1)}$ cubic in y and hence a $\tilde{U}^{(1)}$ of quadratic form, is analogous to that studied by Cessi *et al.* (1987) in a barotropic model of the recirculation and Cessi (1988) in a two-layer baroclinic model. It differs from theirs, however, in our choice of boundary conditions:

$$\tilde{\psi}^{(i)} = 0 \qquad \text{at } y = 0 \tag{16a}$$

$$\tilde{\psi}^{(i)} = \mathbf{e}_i^* \cdot (\Psi_1, \Psi_2, 0)^{\mathrm{T}} \qquad \text{at } y = -l_3 \tag{16b}$$

with $\Psi_{1,2} = \lim(y \to l_3^-)\, \psi_{\mathrm{II},2}$ obtained from Eqs. (5).

Equation (16b) should be contrasted with that adopted by Cessi *et al.* who set $\psi^{(i)}$ to zero at the southern edge of the recirculation. Instead here the solution is matched to the baroclinic fringe Eqs. (5) found by MN.

The pseudo-baroclinic components $\tilde{\psi}^{(2)}$ and $\psi^{(3)}$ exhibit confined boundary layers, whose widths are the same order as the corresponding Rossby radii, typically much less than the meridional extent of the recirculation.

Figure 8 shows the structure of the boundary current north of $y = -l_3$ implied by Eqs. (15) and (16) for $C_1' = -1/4$, $C_3' = 0{\cdot}4$ as in Fig. 7(c). The solution does not have boundary layer form and, in contrast with the sections shown in Fig. 7, the relative vorticity is important over the whole of the recirculation. In Fig. 8(a) the interface displacements are plotted; it can be seen that relative vorticity arrests the downward plunge of the isopycnals, allowing them to turn upward as the westward flowing recirculation gives way to the strong eastward flowing jet stream. The presence of relative vorticity allows the uniformity of potential vorticity in the interior layer to be maintained even though the layer is becoming thinner as f increases moving northwards. The interfaces return to their reference depths at the axis of the Stream at $y = 0$.

The zonal velocities normal to the section in the three layers are plotted in Fig. 8(b). As in Fig. 7 the velocities are scaled with respect to β/F. Again taking $F^{-1/2}$ to be 30 km and $\beta = 2\times10^{-11}\mathrm{m}^{-1}\mathrm{s}^{-1}$, velocities reach $1{\cdot}5\,\mathrm{m\,s}^{-1}$ at the axis of the Stream in the upper layer falling to 5–10 $\mathrm{cm\,s}^{-1}$ at depth. The jet is broad at the surface becoming narrower with depth; the zero current line approaches the axis of the Stream with depth and thus the abyssal flow can run counter to the surface flow. Note that the net zonal transport in layer three is zero since there is no flow south of $y = -l_3$.

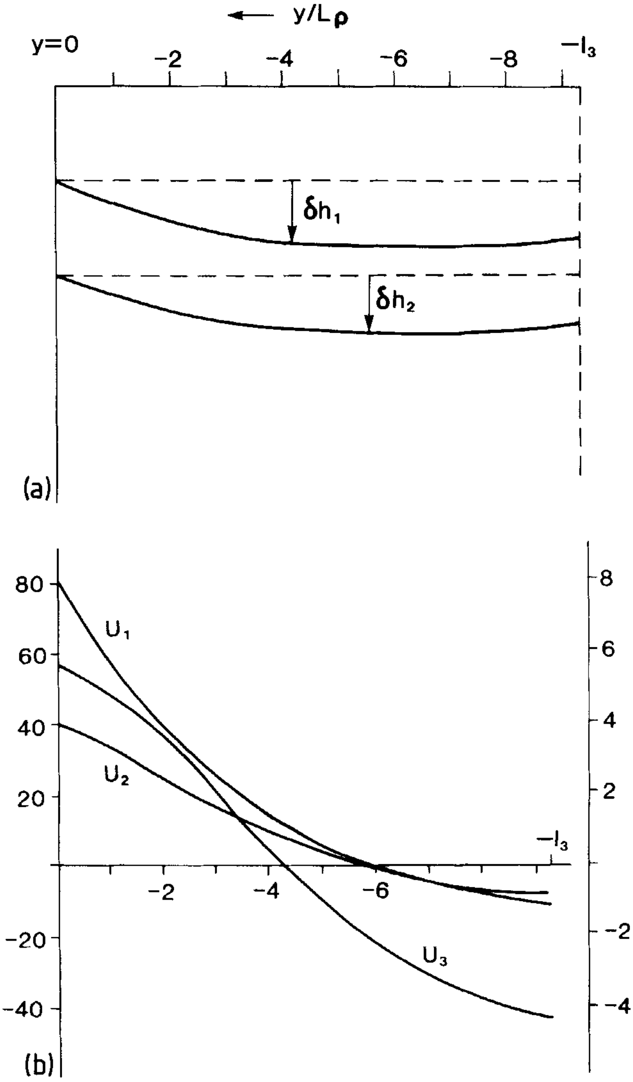

Figure 8. The structure of the northern boundary current, the analogue of the separated Gulf Stream, between $y = -l_3$ and the axis of the Stream at $y = 0$, obtained by solving Eqs. (15) and (16). The solution has been plotted for the case $C_1' = -0{\cdot}25$, $C_3' = 0{\cdot}4$ and $\alpha = 1/8$, as in Fig. 7(c). The y axis is in units of Rossby radii $L_\rho = F^{-1/2}$; thus $y = -l_3$ is some 270 km south of the axis of the Stream if L_ρ is taken to be 30 km. (a) The interfacial displacements $\delta h_1 = (f_0/g')(\psi_1 - \psi_2)$ and $\delta h_2 = (f_0/g')(\psi_2 - \psi_3)$. (b) The velocities normal to the section in the three layers; in units of β/F. The scaled axis for U_1 and U_2 is on the left, that for U_3 is on the right. Positive values indicate eastward velocities.

4. Conclusions

We have seen how the baroclinic Fofonoff gyre, homogenized to a uniform value of potential vorticity, provides a useful reference solution from which to interpret observations of the subtropical recirculation. If attention is focused on the interior of the gyre where relative vorticity is unimportant, then the quasi-geostrophic assumption may be relaxed and comparison with the hydrographic sections becomes meaningful. Our solution seems to capture the broad character of the 50°W hydrographic section. It provides a quantitative link between the depth of the bowl and the strength of the circulation within it, to the depth of penetration of the surface mode water layer. The theory suggests that the depth of the bowl is sensitive to variations in the depth of the $\sigma = 26{\cdot}6$ isopycnal but that it is not unlikely that the bowl strikes the ocean floor a few hundred kilometres to the south of the axis of the Stream.

The existence of such steady, free solutions allows the possibility of resonant excitation, given an appropriate forcing function. We have proposed that such a forcing function can be provided by the wind-stress curl, as suggested by Behringer *et al.* (1979), and/or diabatic sources of potential vorticity, as suggested by Worthington (1976). Such a resonance of the baroclinic Fofonoff gyre, spun up by potential vorticity sources in the north-west corner of the gyre, might be a mechanism at work in the observed seasonal intensification of the Gulf Stream and its recirculation. Equilibration of the gyre can come about when the accumulated energy is discharged through instability and lateral transfer of potential vorticity.

The consequences of the foregoing picture of the recirculation have been investigated with a three-layer quasi-geostrophic model. It has been shown how changes in the shear across the main thermocline, brought about by changes in the volume of mode waters in the upper layer, affect the flow in the homogenized and abyssal layers below. We find that as the anticyclogenesis proceeds there is a southward shift of the current systems at depth, and an increase in the barotropic recirculation between the axis of the Stream and the latitude at which the bowl of the circulation strikes the ocean floor. It is hoped that the present study may provide a dynamical framework linking observed variations in the baroclinic and barotropic transport with the depth of the main thermocline on the southern flank of the Stream.

Acknowledgments

We would like to thank the Natural Environment Research Council for their support during this study.

References

Behringer, D., Reiger, L. and Stommel, H. 1979 Thermal feedback as a contributing cause of the Gulf Stream. *J. Mar. Res.*, **37**, 699–709

Bower, A. S., Rossby, H. T. and Lillibridge, J. L. 1985 The Gulf Stream—Barrier or Blender? *J. Phys. Oceanogr.*, **15**, 24–32

Cessi, P., Ierley, G. R. and Young, W. R. 1987 A model of the inertial recirculation driven by potential vorticity anomalies. *ibid.*, **17**, 1640–1652

Cessi, P. 1988 A stratified model of the inertial recirculation. *ibid.*, **18**, 662–682

Fofonoff, N. P. 1954 Steady flow in a frictionless homogeneous ocean. *J. Mar. Res.*, **13**, 254–262

Fu, L., Vazquez, J. and Parke, M. E. 1986 Seasonal variability of the Gulf Stream from satellite altimetry. *J. Geophys. Res.*, **92-C1**, 749–754

Greatbatch, R. J. 1987 A model for the inertial recirculation of a gyre. *J. Mar. Res.*, **45,** 601–634

Halkin, D. and Rossby, T. 1985 The structure and transport of the Gulf Stream at 73 W. *J. Phys. Oceanogr.*, **15,** 1439–1452

Hogg, N. G. 1983 A note on the deep circulation of the western North Atlantic: its nature and causes. *Deep Sea Res.*, **30,** 945–961

Hogg, N. G., Pickart, R. S., Hendry, R. M. and Smethie, W. J. Jr. 1986 The northern recirculation gyre of the Gulf Stream. *ibid.*, **33,** 1139–1165

Luyten, J. and Stommel, H. 1982 Recirculation reconsidered. *J. Mar. Res.*, **40,** 407–426

McCartney, M. S. 1982 The subtropical recirculation of mode waters. *ibid.*, **40,** 427–464

McCartney, M. S., Worthington, L. V. and Raymer, M. E. 1980 Anomalous water mass distributions at 55°W in the North Atlantic in 1977. *ibid.*, **38**, 147–172

Marshall, J. C. 1986 'Wind-driven ocean circulation theory—steady free flow'. Pp. 225–245 in *Large-scale transport processes in the oceans and atmosphere.* NATO ASI series, **190**

Marshall, J. C. and Nurser, A. J. G. MN 1986 Steady, free circulation in a stratified, quasi-geostrophic ocean. *J. Phys. Oceanogr.*, **16,** 1799–1813

Nurser, A. J. G. 1988 The distortion of a baroclinic Fofonoff gyre by wind forcing. *ibid.*, **18**, 243–257

Rhines, P. B. and Young, W. R. 1982 A theory of wind-driven circulation. I. Mid-ocean gyres. *J. Mar. Res.*, **40,** 559–596

Richardson, P. L. 1985 Average velocity transport of the Gulf Stream near 55 W. *ibid.*, **43,** 83–111

Schmitz, W. J. 1980 Weakly depth-dependent segments of the North Atlantic circulation. *ibid.*, **38,** 111–133

Schmitz, W. J. and Holland, W. R. 1986 Observed and modelled mesoscale variability near the Gulf Stream and Kuroshio. *J. Geophys. Res.*, **91-C8,** 9624–9638

Schmitz, W. J. and McCartney, M. S. 1982 An example of long-term variability for subsurface current and hydrographic patterns in the western North Atlantic. *J. Mar. Res.*, **40,** 707–726

Woods, J. D. and Barkmann, W. 1985 A Lagrangian mixed layer model of Atlantic 18 C water formation. *Nature*, **319,** 574–576

Worthington, L. V. 1972 'Anticyclogenesis in the oceans as a result of outbreaks of continental polar air'. Pp. 169–78 in *Studies in Physical Oceanography—A tribute to George Wust on his 80'th birthday.* Vol. 1, A. L. Gordon, Ed., Gordon and Breach, New York

1976 *On the North Atlantic circulation.* Johns Hopkins Oceanographic Studies, Vol. VI.

1977 Intensification of the Gulf Stream after the winter of 1976–1977. *Nature*, **270**, 415–417

1982 North Atlantic circulation and water mass formation. *J. Mar. Res.*, **40,** xiii–xxii